
Transformer Compression via Subspace Projection

Yuxuan Hu
Renmin University of China
huyuxuan1999@ruc.edu.cn

Jing Zhang
Renmin University of China
zhang-jing@ruc.edu.cn

Chen Zhao
Renmin University of China
2021201645@ruc.edu.cn

Cuiping Li
Renmin University of China
licuiping@ruc.edu.cn

Hong Chen
Renmin University of China
chong@ruc.edu.cn

Abstract

We propose TCSP, a novel method for compressing a transformer model by focusing on reducing the hidden size of the model. By projecting the whole transform model into a subspace, we enable matrix operations between the weight matrices in the model and features in a reduced-dimensional space, leading to significant reductions in model parameters and computing resources. To establish this subspace, we decompose the feature matrix, derived from different layers of sampled data instances, into a projection matrix. For evaluation, TCSP is applied to compress T5 and BERT models on the GLUE and SQuAD benchmarks. Experimental results demonstrate that TCSP achieves a compression ratio of 44% with at most 1.6% degradation in accuracy, surpassing or matching prior compression methods. Furthermore, TCSP exhibits compatibility with other methods targeting filter and attention head size compression.

1 Introduction

The transformer model [1] is widely used in Natural Language Processing as well as other domains such as Computer Vision [2, 3, 4] and Speech Recognition [5, 6, 7]. Despite its impressive performance, the large size of transformer models and the high inference latency limit their practical deployment. To address this challenge, model compression techniques including pruning [8, 9, 10, 11, 12, 13] and low-rank decomposition [14, 15, 16, 17] have been proposed to reduce model parameters and improve inference speed while ensuring that the performance of the compressed model is not significantly disturbed.

The transformer model consists of a series of weight matrices that are determined by the hidden size d , attention head size d_h in the multi-head attention layers, and the number of filters d_f in the feed-forward network layers. Existing compression methods primarily focus on reducing the attention head size d_h [14, 8, 13] and the number of filters d_f [8, 13], or performing matrix decomposition to transform $d \times d$ matrices into two $d \times k$ matrices [14, 15, 16]. However, none of these methods directly address the reduction of the hidden size d . Although CoFi [13], a pruning method, attempts to compress d , it can only achieve a 1% reduction while keeping model performance.

This paper introduces a novel method, named **Transformer Compression via Subspace Projection** (TCSP), for compressing transform models by reducing the hidden size. By projecting the transformer model into a subspace, TCSP achieves this compression. To create this subspace, we employ low-rank factorization to decompose the feature matrix derived from sampled data instances into a projection matrix. Specifically, we gather multiple data instances, pass each through the transformer model to obtain their respective features from different layers, and concatenate them to form a feature matrix. Decomposing this matrix yields the projection matrix, which allows us to project the model into a

subspace, resulting in a significant reduction in model parameters. Furthermore, TCSP can be easily combined with other compression methods that reduce attention head size and the number of filters, ensuring compatibility. Although low-rank factorization is employed in TCSP, it is considered a sub-technique to achieve the primary goal of reducing hidden size.

Our contributions can be summarized as follows:

- We take a fresh perspective on model compression by reducing the hidden size of the transformer model, which has been rarely explored before.
- We propose the TCSP technique to achieve the compression goal. TCSP decomposes the feature matrix derived from sampled data instances into a projection matrix, which is then used to project the transformer model into a subspace. In addition, TCSP is compatible with other compression methods, such as reducing the multi-head attention size and the number of filters, which could further speed up inference.
- Experimental results on two widely-used benchmarks, GLUE and SQuAD, show that TCSP can compress 44% of the parameters of both T5 and BERT within 1.6% accuracy loss, surpassing or matching prior compression methods.

2 Related Work

The transformer model is a general model that has been widely used in the fields of deep learning. To improve inference speed and reduce memory overhead, different approaches have been proposed to compress the transformer. Previous research [18] categorize these approaches into five distinct categories: quantization [19, 20, 21], pruning [8, 9, 10, 11, 12, 13], knowledge distillation [22, 23], low-rank factorization [14, 15, 16, 17], and weight sharing [24, 25]. These five types of methods are orthogonal to each other. In this work, we focus on exploring low-rank factorization and pruning approaches as means to directly reduce the number of parameters in fine-tuned task-specific models. We do not delve into Knowledge distillation and weight sharing, as they involve training models from scratch. We do not cover quantization, which compresses models based on storage considerations.

Low-Rank Factorization for Transformer. In recent years, various low-rank decomposition methods have been proposed specifically for Transformers. Ma et al. [26] introduce a block term tensor decomposition approach to decompose the multi-head attention in Transformers. Noach et al. [27] propose a two-stage method for Transformer compression, where they first employ SVD to decompose Transformer’s weight matrix and then fine-tune the model using knowledge distillation. However, direct SVD-based compression of the weight matrix assumes that it possesses low-rank properties, which may not always hold for Transformers. To address this issue, Chen et al. [14] propose a data-aware low-rank factorization method. This method minimizes the reconstruction error of the matrix multiplication between each weight matrix and its corresponding input feature matrix rather than directly minimizing the reconstruction error of the weight matrix itself. Hsu et al. [15] and Hua et al. [16] propose FWSVD and TFWSVD, respectively, which utilize Fisher information to measure the contribution of different parts of the weight matrix to model performance during the SVD process, achieving improved results compared to direct SVD. Alternatively, Tahaei et al. and Edalati et al. [28, 29] employ Kronecker decomposition to preserve the matrix rank and successfully compress models like BERT and GPT2.

Pruning for Transformer. Pruning is a commonly used technique for eliminating unnecessary parameters in the model. Existing pruning methods can be broadly divided into two categories: unstructured pruning and structured pruning. Unstructured pruning aims to remove unimportant scalar values in model’s parameters. Various unstructured pruning approaches have been proposed for Transformer, such as magnitude-based [30], first-order [31], second-order [32], and lottery ticket hypothesis [33]. Although unstructured pruning algorithms can remove many redundant parameters while ensuring accuracy, compressed models require specific sparse data structures and hardware support to take advantage of unstructured pruning. For this reason, structure pruning approaches [8, 9, 10, 11, 12, 13] are proposed to remove weight blocks in the transformer model, including entire transformer layers, attention heads, and filters. Unlike unstructured pruning, structure pruning can accelerate inference speed and reduce memory overhead without specialized data structure and hardware.

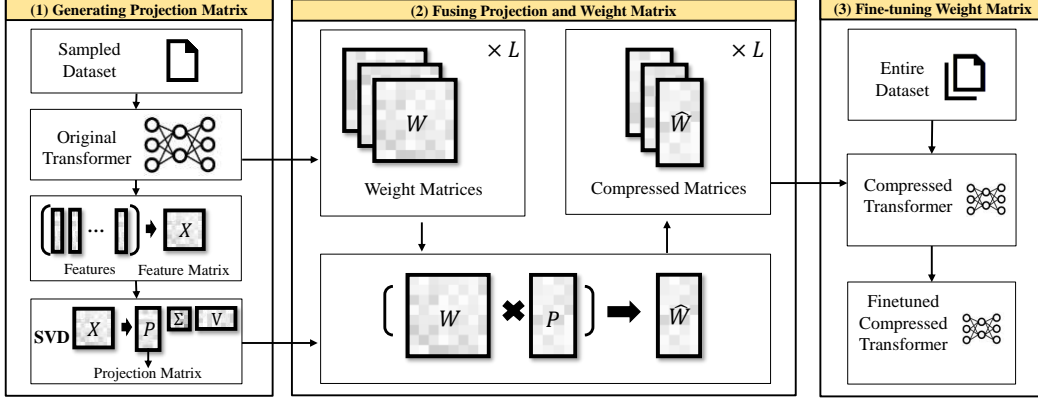


Figure 1: Workflow of Transformer Compression via Subspace Projection (TCSP).

3 Overview

3.1 Preliminary: Transformer Architecture

We take T5 [34] as an example of the transformer model to present the proposed TCSP, although it can be easily extended to other transform models such as BERT [35] and GPT [36].

A transformer model comprises a stack of blocks, each containing a multi-head attention (MHA) layer, an optional cross-attentive (CA) layer, and a feed-forward network (FFN) layer.

Multi Head Attention (MHA). In a transformer encoder, each MHA layer consists of H attention heads that facilitate interactions between tokens, with a pre-normalization step. Other transform models such as BERT adopt post-normalization after the MHA layer.

$$x_M = x + \text{MHA}(x_n), \quad x_n = \text{norm}(x), \quad \text{MHA}(x_n) = \sum_{i=1}^H \text{Att}^{(i)}(x_n), \quad (1)$$

$$\text{Att}^{(i)}(x_n) = W_O^{(i)\top} W_V^{(i)} x_n \cdot \text{Softmax}((W_K^{(i)} x_n)^\top (W_Q^{(i)} x_n) / \sqrt{d}), \quad (2)$$

where $\text{norm}(x)$ represents the normalization function such as LayerNorm and RMSNorm, $W_Q, W_K, W_V, W_O \in \mathbb{R}^{d_h \times d}$ are the parameters of an MHA layer, denoting the query, key, value, and output matrices, respectively. Here d denotes the hidden size, and $d_h = d/H$ denotes the attention head size.

In a transformer decoder, a CA layer is added after the MHA layer. The CA layer closely resembles the MHA, with one only distinction: the feature matrices multiplied by W_Q and W_K in the CA layer are sourced from the output of the Transformer encoder. Further information on the CA layer can be found in Appendix A.

Feed Forward Network (FFN). Following each MHA layer, there is an FFN layer that takes x_M as input and generates x_F as output:

$$x_F = x_M + \text{FFN}(x_n), \quad x_n = \text{norm}(x_M), \quad \text{FFN}(x_n) = W_D^\top \sigma(W_U x_n), \quad (3)$$

where σ is the activation function, and $W_U, W_D \in \mathbb{R}^{d_f \times d}$ are the parameters of the FFN layer, which correspond to the up and down matrices, respectively. Here d_f indicates the number of filters.

3.2 Basic Idea of TCSP: Subspace Projection

The basic idea of Transformer Compression via Subspace Projection (TCSP) is to project the Transformer model into a suitable subspace via matrix fusion. To provide a clearer explanation, we take the linear regression model as an example. Here we denote the original model \mathcal{F} as:

$$\mathcal{F}(x) = Wx, \quad (4)$$

where $W \in \mathbb{R}^{1 \times d}$, $x \in \mathbb{R}^d$.

Assume that the input x of the model is distributed in a k -dimensional subspace. In other words, there exists a projection matrix $P \in \mathbb{R}^{d \times k}$ such that every x in the dataset satisfies $x = P\hat{x}$, where $\hat{x} \in \mathbb{R}^k$. Thus, we have,

$$\hat{\mathcal{F}}(\hat{x}) = (WP)\hat{x} = \hat{W}\hat{x}, \quad (5)$$

where $\hat{W} = WP \in \mathbb{R}^{1 \times k}$ represents the compressed weight matrix, $\hat{x} \in \mathbb{R}^k$. In this way, we project the original model from a d -dimensional space into a reduced k -dimensional subspace. We will elaborate on how to extend this method to the transformer model.

Workflow of TCSP. The proposed TCSP comprises three stages, as illustrated in Figure 1. Firstly, given the training data and the original transformer model (e.g., a fine-tuned T5), we sample a subset of the training data, feed it into the transformer model to obtain the feature matrix X , and employ SVD on X to derive the projection matrix P . Then, we project the weight matrices $\{W\}$ of the original transformer to a subspace via the fusion of the model’s weight matrices and the projection matrix, resulting in $\{\hat{W}\}$. Finally, following prior work [14, 15, 16], we fine-tune the compressed transformer with the entire training data.

4 Methodology

4.1 Generating Projection Matrix

Motivated by the fact that features produced by the transformer model usually tend to reside in a low-dimensional subspace, our objective is to carry out the forward pass of the transformer model in the low-dimensional subspace. To achieve this, the initial step of TCSP focuses on determining the subspace where the features are located. This can be formalized as an optimization problem:

$$\arg \min_P \mathbb{E}_{x \in \mathbb{D}} \left(\sum_{i=1}^N \|L^{(1 \sim i)}(x) - PP^\top L^{(1 \sim i)}(x)\|_F^2 \right) \quad \text{s.t.} \quad P^\top P = \mathbf{I}, \quad (6)$$

where N denotes the number of layers in the transformer, $L^{(i)}$ represents the i -th layer in the transformer model, which can correspond to different components, such as the MHA or the FFN layer. $L^{(1 \sim i)} = L^{(i)} \circ \dots \circ L^{(2)} \circ L^{(1)}$ represents the composite function that is formed by sequentially applying the transformations from the first layer to the i -th layer. $L^{(1 \sim i)}(x)$ refers to the application of the composition function $L^{(1 \sim i)}$ on the input x , resulting in its corresponding feature. \mathbf{I} is an identity matrix, and P is the desired projection matrix. For a given projection matrix P , $P^\top x$ can be interpreted as projecting x from the original space into the subspace corresponding to the matrix P , while $PP^\top x$ can be viewed as projecting $P^\top x$ from the subspace back into the original space. Therefore, we can use $x - PP^\top x$ to measure whether the vector x belongs to the subspace.

Eq. 6 is equivalent to the following equation, the proof of which is shown in Appendix B.

$$\arg \min_P \|X - PP^\top X\|_F^2 \quad \text{s.t.} \quad P^\top P = \mathbf{I}, \quad (7)$$

where

$$X = [L^{(1)}(x_1), \dots, L^{(1)}(x_M), L^{(1 \sim 2)}(x_1), \dots, L^{(1 \sim 2)}(x_M), L^{(1 \sim N)}(x_1), \dots, L^{(1 \sim N)}(x_M)]. \quad (8)$$

Let l_m denote the sequence length of the m -th data instance, and d denote the hidden size. Consequently, the shape of X can be expressed as $d \times (N \times \sum_{m=1}^M l_m)$, where N is the number of layers, and M is the number of the sampled data instances.

Such an optimization problem in Eq. 7 can be well solved by SVD [37].

$$U, \Sigma, V^\top = \text{SVD}(X), \quad (9)$$

where U and V are two orthogonal matrices, and Σ is a diagonal matrix.

Then, the first k columns of the matrix U (i.e., the top- k important eigenvectors of the feature matrix X) compose the desired projection matrix P .

$$P = U_{:, :k} \quad (10)$$

Appendix G.1 describes the process of generating the projection matrix P . Notably, although we sample a subset of data instances for computing feature matrix X , the size of X is still large, resulting in a significant overhead of SVD. To mitigate this, we only select a subset of columns from X to create a submatrix for SVD. Following previous work [14, 8], we approximate the SVD by sampling 2,000 tokens, which corresponds to the number of columns in matrix X . In the experiments, we examine the impact of the number of sampled tokens on the performance of TCSP.

4.2 Fusing Projection and Weight Matrix

Once the projection matrix P for the the transformer model has been obtained, we can construct an approximation of the original model within the subspace using the projection matrix. The basic idea behind this is to fuse the projection matrix with the weight matrices of the transformer.

Given an input x , we pass it through the transformer model starting from the first layer to the last N -th layer, resulting in the corresponding feature vector $L^{(1\sim N)}(x)$. According to Eq.6, we can use the projection matrix P to add dimensionality reduction and dimensionality enhancement operations between each layer, while preserving the final outcome, as shown in the following equation,

$$L^{(1\sim N)}(x) = L^{(N)} \circ \dots \circ L^{(2)} \circ L^{(1)} \quad (11)$$

$$\approx U \circ D \circ L^{(N)} \circ \dots \circ L^{(2)} \circ U \circ D \circ L^{(1)} \circ U \circ D(x) \quad (12)$$

$$\approx U \circ \hat{L}^{(N)} \circ \dots \circ \hat{L}^{(2)} \circ \hat{L}^{(1)} \circ D(x) \quad (13)$$

$$\approx P \hat{L}^{(1\sim N)}(P^\top x), \quad (14)$$

where $U(x) = Px$ represents the dimensionality enhancement operation, $D(x) = P^\top x$ represents the dimensionality reduction operation, $\hat{L}^{(i)} = D \circ L^{(i)} \circ U$ is the projected layer, and $\hat{L}^{(1\sim N)} = \hat{L}^{(N)} \circ \dots \circ \hat{L}^{(2)} \circ \hat{L}^{(1)}$ is the projected model.

According to Section 3.1, any original layer $L^{(i)}(x)$ can be formulated as:

$$L(x) = x + \text{Layer}(\text{norm}(x)), \quad (15)$$

where the function ‘‘Layer’’ can be instantiated by various components such as MHA, CA, and FFN. The projected layer \hat{L} operates on a k -dimensional feature \hat{x} as input and produces a corresponding k -dimensional feature $\hat{L}(\hat{x})$, i.e.

$$\hat{L}(\hat{x}) = P^\top (P\hat{x} + \text{Layer}(\text{norm}(P\hat{x}))) = \hat{x} + P^\top \text{Layer}(\text{norm}(P\hat{x})). \quad (16)$$

Compared with the d -dimensional input and output vectors of the original layer $L(x)$, the projected layer $\hat{L}(\hat{x})$ in Eq.16 reduces the dimensions of the layer’s input and output to k . However, this reduction in dimensionality does not alleviate the computational effort. Therefore, we propose two methods to compress the parameters within the projected layer: (1) Matrix fusion, which merges the multiple consecutive matrix multiplications into a single matrix. (2) Normalization function reconstruction, which is used to swap the computational order of matrix operations and normalized functions to increase the chance of matrix fusion. Next, we first explain the normalization function

reconstruction and then discuss how the matrix fusion technique can be employed to compress the MHA and FFA layers.

Normalization Function Reconstruction. Within the projected layer \hat{L} as shown in Eq.16, we encounter the computation of $\text{norm}(P\hat{x})$. Additionally, we know that the operation following $\text{norm}(P\hat{x})$ is a matrix multiplication. Thus, if we can find a new matrix \hat{P} along with a normalization function norm that satisfies $\text{norm}(P\hat{x}) = \hat{P}\text{norm}(\hat{x})$, we can compress the parameters of the transformer model by fusing the matrix \hat{P} with the subsequent matrix.

The normalization function in T5 is RMSNorm [38]:

$$\text{norm}(x) = \gamma \frac{x}{\sqrt{\frac{1}{d}\|x\|}}. \quad (17)$$

Therefore, we have

$$\text{norm}(P\hat{x}) = \gamma \frac{P\hat{x}}{\sqrt{\frac{1}{d}\|P\hat{x}\|}} = \left(\sqrt{\frac{d}{k}}\gamma P\right) \mathbf{I} \frac{\hat{x}}{\sqrt{\frac{1}{k}\|\hat{x}\|}} = \hat{P}\text{norm}(\hat{x}), \quad (18)$$

where $\hat{P} = \sqrt{\frac{d}{k}}\gamma P$, $\text{norm}(\hat{x}) = \mathbf{I} \frac{\hat{x}}{\sqrt{\frac{1}{k}\|\hat{x}\|}}$ (note that $\|\hat{x}\| = \|P\hat{x}\|$).

By incorporating Eq.18 into Eq.16, we can define

$$\text{Layer}(\hat{x}) = P^\top \text{Layer}(\hat{P}\text{norm}(\hat{x})) = P^\top \text{Layer}(\hat{P}\hat{x}_n), \quad (19)$$

where $\text{norm}(\hat{x})$ is abbreviated as \hat{x}_n .

For detailed information on reconstructing other normalization functions such as LayerNorm [39] and BatchNorm [40], please refer to the appendix C. The post-normalization reconstruction is also explained in appendix C.

MHA Layer Compression. We can compress the transformer model’s parameters by fusing multiple consecutive matrix multiplications into a single matrix. For the MHA layer, we have

$$\text{MHA}(\hat{x}_n) = \sum_{i=1}^H P^\top W_O^{(i)\top} W_V^{(i)} \hat{P}\hat{x}_n \cdot \text{Softmax}((W_K^{(i)} \hat{P}\hat{x}_n)^\top (W_Q^{(i)} \hat{P}\hat{x}_n)/\sqrt{d}) \quad (20)$$

$$= \sum_{i=1}^H \hat{W}_O^{(i)\top} \hat{W}_V^{(i)} \hat{x}_n \cdot \text{Softmax}((\hat{W}_K^{(i)} \hat{x}_n)^\top (\hat{W}_Q^{(i)} \hat{x}_n)/\sqrt{d}), \quad (21)$$

where $\hat{W}_O^{(i)} = W_O^{(i)}P$, $\hat{W}_V^{(i)} = W_V^{(i)}\hat{P}$, $\hat{W}_K^{(i)} = W_K^{(i)}\hat{P}$, $\hat{W}_Q^{(i)} = W_Q^{(i)}\hat{P}$. The shape of these matrices is transformed from $d_h \times d$ to $d_h \times k$, resulting in a reduction of k/d of the original number of parameters. We introduce the CA layer compression in Appendix E.

FFN Layer Compression. For the FFN layer, we have

$$\text{FFN}(\hat{x}_n) = P^\top W_D^\top \sigma(W_U \hat{P}\hat{x}_n) = \hat{W}_D^\top \sigma(\hat{W}_U \hat{x}_n), \quad (22)$$

where $\hat{W}_D = W_D P$, $\hat{W}_U = W_U \hat{P}$, which has the same compression rate as the MHA Layer. The complete compression process is shown in Appendix G.2.

4.3 Combining TCSP with Other Compression Algorithms

TCSP compresses the hidden size d , and we can further compress the number of filters d_f and attention head size d_h by the prior pruning and low-rank factorization methods.

Filter Pruning. We can remove the filters in the FFN layer by pruning. Following prior work [13, 8], we introduce mask variables $\text{diag}(m)$ into the FFN layer, where m indicates which filters in the FFN layer are to be retained.

$$\text{FFN}(x; m) = W_D^\top \text{diag}(m) \sigma(W_U x). \quad (23)$$

Then the pruning problem can be formalized as an optimization problem on the mask.

$$\arg \min_m \mathcal{L}(m) \quad s.t. \quad \text{cost}(m) \leq C. \quad (24)$$

Our proposed TCSP method only involves the forward computation process of the model. However, most prior methods find the optimal mask by leveraging the derivative of the loss function with respect to the mask variable $\frac{\partial \mathcal{L}}{\partial m}$. As a result, TCSP cannot be directly integrated into the same framework as previous pruning algorithms. To address this, we propose TCSP-pruning, a filter pruning algorithm that exclusively relies on the forward process of the model, enabling the unifying of the pruning algorithm into the TCSP framework.

TCSP-pruning employs a greedy algorithm to remove the least important filter at each step based on the following score function:

$$\text{score}(i) = |W_{D,i}| * (\mathbb{E}[\sigma(W_{U,i}x)] + \text{std}[\sigma(W_{U,i}x)]), \quad (25)$$

where $\text{score}(i)$ represents the significance of the i -th filter. We believe that the importance of the i -th filter is influenced by the factors such as the norm of $W_{D,i}$ (the weight matrix associated with the i -th filter), the average activation value, and the variance of activation values. The pseudo-code of TCSP-pruning is shown in the Appendix G.3.

Head Size Compression. Based on the low-rank property of data distribution, we can further compress the head size of the MHA layer. The objective can be expressed as:

$$\arg \min_M \mathbb{E}_x \|(W_K x)^\top (W_Q x) - (W_K x)^\top M (W_Q x)\|_F^2 \quad s.t. \quad \text{rank}(M) = k, \quad (26)$$

$$\arg \min_M \mathbb{E}_x \|W_O^\top W_V x - W_O^\top M' W_V x\|_F^2 \quad s.t. \quad \text{rank}(M') = k. \quad (27)$$

DRONE [14] gives the solution to the above two optimization problems. Assuming that the optimal solution obtained from the first optimization problem is M^* . Afterward, we decompose M^* into the product of two matrices $M^* = U_M^\top V_M$ through SVD. Then, we can compress matrices W_Q, W_K through U_M and V_M ($\hat{W}_K = U_M W_K, \hat{W}_Q = V_M W_Q$). The second problem is addressed in the same way. We can also formalize Eq.7 as $\arg \min_M \|X - MX\|_F^2 \quad s.t. \quad \text{rank}(M) = k$, but the optimal solution obtained by both formulas is the same.

5 Experiment

5.1 Experimental Setup

To evaluate our method, we first fine-tune T5_{base} and BERT_{base} on the training data of each task of the GLUE[41] and SQuAD [42] benchmarks to obtain the baseline models, and then adopt the proposed TCSP or the comparison compression methods to compress these baseline models. On each task, for TCSP, we sample 2000 instances from its training data to produce the project matrix, using it to compress the baseline models and finally fine-tune the compressed models using the entire training data. For the GLUE benchmark, We report accuracy for the MNLI [43], QQP [44], QNLI [41], and SST2 [45] tasks, as well as F1 score and spearman correlation for the MRPC [46] and STSB [41] tasks. For the SQuAD benchmark, we report the F1 score. For more comprehensive information regarding the experimental setup, please refer to Appendix F.

Table 1: Performance of TCSP on $T5_{\text{base}}$ and $BERT_{\text{base}}$ with various compression rate. ‘‘Avg. Diff’’ refers to the average accuracy difference observed before and after applying model compression on the GLUE and SQuAD datasets. ‘‘Speed Up’’ represents the rate of inference time speedup achieved by ‘‘w TCSP{25%, 25%}’’ compared to the baseline model. ‘‘ft.’’ denotes fine-tuning.

	MNLI	QQP	QNLI	SST-2	STS-B	MRPC	SQuAD _{1.1}	SQuAD _{2.0}	Avg. Diff
$T5_{\text{base}}$	86.8	91.4	93.2	94.5	90.0	91.9	88.6	79.3	
w TCSP {25%, 0%}	85.0	90.1	91.4	93.0	88.9	89.1	83.9	71.9	
w TCSP {25%, 0%} + ft.	86.2	91.2	92.5	93.2	90.1	91.3	86.8	78.0	-0.6/-1.3
w TCSP {25%, 25%}	83.5	88.0	90.8	91.4	86.6	90.4	79.2	66.9	
w TCSP {25%, 25%} + ft.	85.5	90.7	91.8	92.8	89.5	91.5	87.3	77.7	-1.0/-1.5
Speed Up	$\times 1.25$	$\times 1.06$	$\times 1.08$	$\times 1.36$	$\times 1.22$	$\times 1.25$	$\times 1.15$	$\times 1.20$	
$BERT_{\text{base}}$	84.4	91.1	91.4	92.2	88.4	89.9	88.5	75.8	
w TCSP {25%, 0%}	31.8	68.7	49.5	49.2	68.5	1.0	13.5	11.2	
w TCSP {25%, 0%} + ft.	83.7	91.0	91.0	92.2	88.5	90.1	86.7	76.6	-0.2/-0.5
w TCSP {25%, 25%}	31.8	67.6	49.8	49.1	67.5	0.0	12.9	10.6	
w TCSP {25%, 25%} + ft.	83.5	90.8	90.6	91.9	87.7	89.1	87.7	76.0	-0.6/-0.3
Speed Up	$\times 1.16$	$\times 1.02$	$\times 1.62$	$\times 2.36$	$\times 1.96$	$\times 3.93$	$\times 1.36$	$\times 1.36$	

Table 2: Performance comparison with prior compression methods using $BERT_{\text{base}}$ as the baseline.

	Sajjad et al.(33.3%)	Kwon et al.(40%)	DRONE(-)	FWSVD(40%)	TFWSVD(40%)	TCSP(40%)
QQP	90.6(-0.5)	90.4(-0.6)	90.1(-0.8)	87.6*(-0.2)	86.9*(-0.9)	<u>90.8(-0.3)</u>
QNLI	89.7(-1.4)	90.0(-1.4)	89.3(-2.1)	89.5(-1.8)	90.3(-1.0)	<u>90.6(-0.8)</u>
SST-2	90.6(-1.8)	<u>92.5(-1.1)</u>	90.8(-1.5)	91.2(-1.8)	91.1(-1.9)	<u>91.1(-1.1)</u>
MRPC	79.4(-8.6)	85.3(-1.0)	88.0(-1.5)	88.0(+0.6)	89.0(+1.6)	<u>89.1(-0.8)</u>

5.2 Performance Evaluation

Table 1 shows the accuracy results of $T5_{\text{base}}$ and $BERT_{\text{base}}$ with different compression rates. The proposed TCSP can reduce the hidden size d . Additionally, in Section 4.3, we introduce a filter pruning method that can reduce the number of filters d_f . Moreover, the existing DRONE [14] can compress the attention head size d_h . In $\text{TCSP}\{a\%, b\%\}$, the notation $a\%$ denotes the compress rate of hidden size, while $b\%$ denotes the compress rate of the attention head size plus the number of filters. Consequently, the overall compression rate of the model is $a\% + b\% - a\% * b\%$.

When employing TCSP with a compression rate of $\{25\%, 0\%\}$ which retains 75% hidden size while preserving the original attention head size and number of filters, we observe that the compressed $T5_{\text{base}}$ and $BERT_{\text{base}}$ models exhibit a maximum drop in accuracy of only 1.3% on the GLUE and SQuAD datasets. Building upon this, We further apply filter pruning and compress the head size, resulting in a model denoted as $\text{TCSP}\{25\%, 25\%\}$. Remarkably, this additional compression does not negatively impact the baseline performance, highlighting the compatibility of TCSP with the filter pruning and attention head size compression methods. Overall, we achieve a compression rate of 44% for both $T5_{\text{base}}$ and $BERT_{\text{base}}$ models with only a 1.6% loss in accuracy. Like prior work [14, 15, 16], fine-tuning is necessary for ensuring performance. For more detailed information on model performance at various compression rates, please refer to Appendix F.5.

5.3 Comparison with Prior Methods

We conduct a comprehensive comparison of TCSP with prior methods, considering both their performance and compression time cost.

Following the setting adopted by Kwon et al. [8], we compare TCSP with prior pruning methods and low-rank factorization methods. The evaluation involves compressing models with compression rate constraints on four tasks within the GLUE benchmark: QQP, QNLI, SST-2, and MRPC. Notably, we conduct this evaluation without employing knowledge distillation. The comparison methods include Sajjad et al. [47], Kwon et al. [8], DRONE [14], FWSVD [15], and TFWSVD [16]. To ensure a fair comparison, we select $BERT_{\text{base}}$ as the baseline model, as it is commonly employed across all the comparison methods. To assess the impact of compression, we compare the amount of accuracy drop

Table 3: Compression time cost comparison with prior compression methods using $BERT_{\text{base}}$ as the baseline evaluated on the MNLI dataset. “# Epochs” represents the number of epochs to fine-tune the model weights on the entire training data.

	DynaBERT [23]	EBERT [11]	BMP [12]	CoFi [13]	Kwon et al. [8]	TCSP
Time cost (hr)	12	5	17	33	0.01	2.16 (0.16 + 2.00)
# Epochs	4	6	20	40	0	2

Table 4: Effect of sampled tokens.

Number of tokens	QQP	QNLI	SST-2	MRPC
1K	91.2	92.3	93.8	91.5
2K	91.2	92.5	93.2	91.3
4K	91.2	92.5	93.7	91.8

Table 5: Effect of SVD

Method	QQP	QNLI	SST-2	MRPC
TCSP-SVD	91.2	92.5	93.2	91.3
TCSP-Random	63.1	49.4	49.0	0.0

experienced by each method since the absolute accuracy of the baseline $BERT_{\text{base}}$ may vary slightly across different papers. The compression rate is indicated in parentheses after each method’s name, except for DRONE, as their paper does not explicitly report the compression rate.

Table 2 presents the performance of the compressed models and the difference from their corresponding baselines for all the compression methods under comparison. The performance of FWSVD and TFWSVD is marked with an asterisk since they use the F1 metric instead of accuracy specifically on the QQP dataset. However, this metric does not impact the comparison of the metric difference. Our method TCSP demonstrates comparable or superior results compared to the prior methods (A lower accuracy drop indicates better performance).

To assess the time cost, we evaluate the performance on the MNLI dataset, which is larger than other datasets in GLUE. Table 3 shows that TCSP requires only 0.16 hours for model compression and an additional 2 hours to model fine-tuning. This indicates that TCSP is significantly faster than most of the comparison methods, with the exception of the pruning method proposed in Kwon et al. [8]. However, the pruning method can be effectively combined with TCSP, allowing for compatibility and further optimization.

5.4 Ablation Study

To prevent the computation of SVD on excessively large matrices, We sample a subset of columns from the feature matrix. In other words, we randomly choose several tokens within each instance to compute the projection matrix. Consequently, we evaluate the effect of the sampled tokens on the compression performance. Table 4 presents the results of this analysis, revealing that satisfactory outcomes can be achieved when the number of tokens (1,000) is greater than the hidden size of the model (768).

Furthermore, we explore the influence of SVD. In Table 5, we replace the projection matrix generated by SVD with a randomly generated matrix and show the experimental results in Table 5. It is observed that using a random matrix for compression significantly diminishes the model’s performance. Therefore, it is necessary to use SVD to compute the projection matrix.

6 Conclusion

This paper proposes TCSP, a method for compressing the transformer model by leveraging subspace projection. TCSP employs SVD on the feature matrix of sampled data instances to derive a projection matrix. By fusing this matrix into the transformer’s weight matrix, we obtain a compressed model. The model is subsequently fine-tuned using the entire dataset. TCSP is applied to both $T5_{\text{base}}$ and $BERT_{\text{base}}$ and evaluated on GLUE and SQuAD datasets. Remarkably, TCSP achieves a compression ratio of 44% while incurring only a 1.6% decrease in accuracy. As TCSP primarily focuses on compressing the hidden size, it can be easily combined with other methods that compress the number of filters and the attention head size, making it highly compatible.

References

- [1] Ashish Vaswani, Noam Shazeer, Niki Parmar, Jakob Uszkoreit, Llion Jones, Aidan N Gomez, Łukasz Kaiser, and Illia Polosukhin. Attention is all you need. *Advances in neural information processing systems*, 30, 2017.
- [2] Alexey Dosovitskiy, Lucas Beyer, Alexander Kolesnikov, Dirk Weissenborn, Xiaohua Zhai, Thomas Unterthiner, Mostafa Dehghani, Matthias Minderer, Georg Heigold, Sylvain Gelly, et al. An image is worth 16x16 words: Transformers for image recognition at scale. *arXiv preprint arXiv:2010.11929*, 2020.
- [3] Ze Liu, Yutong Lin, Yue Cao, Han Hu, Yixuan Wei, Zheng Zhang, Stephen Lin, and Baining Guo. Swin transformer: Hierarchical vision transformer using shifted windows. In *Proceedings of the IEEE/CVF international conference on computer vision*, pages 10012–10022, 2021.
- [4] Hugo Touvron, Matthieu Cord, Matthijs Douze, Francisco Massa, Alexandre Sablayrolles, and Hervé Jégou. Training data-efficient image transformers & distillation through attention. In *International conference on machine learning*, pages 10347–10357. PMLR, 2021.
- [5] Alexei Baevski, Yuhao Zhou, Abdelrahman Mohamed, and Michael Auli. wav2vec 2.0: A framework for self-supervised learning of speech representations. *Advances in neural information processing systems*, 33:12449–12460, 2020.
- [6] Sanyuan Chen, Chengyi Wang, Zhengyang Chen, Yu Wu, Shujie Liu, Zhuo Chen, Jinyu Li, Naoyuki Kanda, Takuya Yoshioka, Xiong Xiao, et al. Wavlm: Large-scale self-supervised pre-training for full stack speech processing. *IEEE Journal of Selected Topics in Signal Processing*, 16(6):1505–1518, 2022.
- [7] Wei-Ning Hsu, Benjamin Bolte, Yao-Hung Hubert Tsai, Kushal Lakhotia, Ruslan Salakhutdinov, and Abdelrahman Mohamed. Hubert: Self-supervised speech representation learning by masked prediction of hidden units. *IEEE/ACM Transactions on Audio, Speech, and Language Processing*, 29:3451–3460, 2021.
- [8] Woosuk Kwon, Sehoon Kim, Michael W Mahoney, Joseph Hassoun, Kurt Keutzer, and Amir Gholami. A fast post-training pruning framework for transformers. *arXiv preprint arXiv:2204.09656*, 2022.
- [9] Ziheng Wang, Jeremy Wohlwend, and Tao Lei. Structured pruning of large language models. In *Proceedings of the 2020 Conference on Empirical Methods in Natural Language Processing (EMNLP)*, pages 6151–6162, Online, November 2020. Association for Computational Linguistics.
- [10] Zi Lin, Jeremiah Liu, Zi Yang, Nan Hua, and Dan Roth. Pruning redundant mappings in transformer models via spectral-normalized identity prior. In *Findings of the Association for Computational Linguistics: EMNLP 2020*, pages 719–730, Online, November 2020. Association for Computational Linguistics.
- [11] Zejian Liu, Fanrong Li, Gang Li, and Jian Cheng. EBERT: Efficient BERT inference with dynamic structured pruning. In *Findings of the Association for Computational Linguistics: ACL-IJCNLP 2021*, pages 4814–4823, Online, August 2021. Association for Computational Linguistics.
- [12] François Lagunas, Ella Charlaix, Victor Sanh, and Alexander Rush. Block pruning for faster transformers. In *Proceedings of the 2021 Conference on Empirical Methods in Natural Language Processing*, pages 10619–10629, Online and Punta Cana, Dominican Republic, November 2021. Association for Computational Linguistics.
- [13] Mengzhou Xia, Zexuan Zhong, and Danqi Chen. Structured pruning learns compact and accurate models. In *Proceedings of the 60th Annual Meeting of the Association for Computational Linguistics (Volume 1: Long Papers)*, pages 1513–1528, 2022.
- [14] Patrick Chen, Hsiang-Fu Yu, Inderjit Dhillon, and Cho-Jui Hsieh. Drone: Data-aware low-rank compression for large nlp models. *Advances in neural information processing systems*, 34:29321–29334, 2021.
- [15] Yen-Chang Hsu, Ting Hua, Sungen Chang, Qian Lou, Yilin Shen, and Hongxia Jin. Language model compression with weighted low-rank factorization. In *International Conference on Learning Representations*, 2022.

- [16] Ting Hua, Yen-Chang Hsu, Felicity Wang, Qian Lou, Yilin Shen, and Hongxia Jin. Numerical optimizations for weighted low-rank estimation on language models. In *Proceedings of the 2022 Conference on Empirical Methods in Natural Language Processing*, pages 1404–1416, Abu Dhabi, United Arab Emirates, December 2022. Association for Computational Linguistics.
- [17] Hao Yu and Jianxin Wu. Compressing transformers: Features are low-rank, but weights are not! *Proceedings of the AAAI Conference on Artificial Intelligence*, 37(9):11007–11015, Jun. 2023.
- [18] Canwen Xu and Julian McAuley. A survey on model compression and acceleration for pretrained language models, 2022.
- [19] Elias Frantar, Saleh Ashkboos, Torsten Hoefler, and Dan Alistarh. Gptq: Accurate post-training quantization for generative pre-trained transformers, 2023.
- [20] Yuhang Li, Ruihao Gong, Xu Tan, Yang Yang, Peng Hu, Qi Zhang, Fengwei Yu, Wei Wang, and Shi Gu. Brecq: Pushing the limit of post-training quantization by block reconstruction. In *International Conference on Learning Representations*, 2021.
- [21] Sehoon Kim, Amir Gholami, Zhewei Yao, Michael W Mahoney, and Kurt Keutzer. I-bert: Integer-only bert quantization. In *International conference on machine learning*, pages 5506–5518. PMLR, 2021.
- [22] Victor Sanh, Lysandre Debut, Julien Chaumond, and Thomas Wolf. Distilbert, a distilled version of BERT: smaller, faster, cheaper and lighter. *CoRR*, abs/1910.01108, 2019.
- [23] Lu Hou, Zhiqi Huang, Lifeng Shang, Xin Jiang, Xiao Chen, and Qun Liu. Dynabert: Dynamic bert with adaptive width and depth. *Advances in Neural Information Processing Systems*, 33:9782–9793, 2020.
- [24] Zhenzhong Lan, Mingda Chen, Sebastian Goodman, Kevin Gimpel, Piyush Sharma, and Radu Soricut. Albert: A lite bert for self-supervised learning of language representations. *arXiv preprint arXiv:1909.11942*, 2019.
- [25] Yingce Xia, Tianyu He, Xu Tan, Fei Tian, Di He, and Tao Qin. Tied transformers: Neural machine translation with shared encoder and decoder. In *Proceedings of the AAAI conference on artificial intelligence*, volume 33, pages 5466–5473, 2019.
- [26] Xindian Ma, Peng Zhang, Shuai Zhang, Nan Duan, Yuexian Hou, Ming Zhou, and Dawei Song. A tensorized transformer for language modeling. *Advances in neural information processing systems*, 32, 2019.
- [27] Matan Ben Noach and Yoav Goldberg. Compressing pre-trained language models by matrix decomposition. In *Proceedings of the 1st Conference of the Asia-Pacific Chapter of the Association for Computational Linguistics and the 10th International Joint Conference on Natural Language Processing*, pages 884–889, 2020.
- [28] Marzieh Tahaei, Ella Charlaix, Vahid Nia, Ali Ghodsi, and Mehdi Rezagholizadeh. Kronecker-BERT: Significant compression of pre-trained language models through kronecker decomposition and knowledge distillation. In *Proceedings of the 2022 Conference of the North American Chapter of the Association for Computational Linguistics: Human Language Technologies*, pages 2116–2127, Seattle, United States, July 2022. Association for Computational Linguistics.
- [29] Ali Edalati, Marzieh Tahaei, Ahmad Rashid, Vahid Nia, James Clark, and Mehdi Rezagholizadeh. Kronecker decomposition for gpt compression. In *Proceedings of the 60th Annual Meeting of the Association for Computational Linguistics (Volume 2: Short Papers)*, pages 219–226, 2022.
- [30] Trevor Gale, Erich Elsen, and Sara Hooker. The state of sparsity in deep neural networks. *arXiv preprint arXiv:1902.09574*, 2019.
- [31] Victor Sanh, Thomas Wolf, and Alexander Rush. Movement pruning: Adaptive sparsity by fine-tuning. *Advances in Neural Information Processing Systems*, 33:20378–20389, 2020.
- [32] Eldar Kurtic, Daniel Campos, Tuan Nguyen, Elias Frantar, Mark Kurtz, Benjamin Fineran, Michael Goin, and Dan Alistarh. The optimal BERT surgeon: Scalable and accurate second-order pruning for large language models. In *Proceedings of the 2022 Conference on Empirical Methods in Natural Language Processing*, pages 4163–4181, Abu Dhabi, United Arab Emirates, December 2022. Association for Computational Linguistics.
- [33] Jonathan Frankle and Michael Carbin. The lottery ticket hypothesis: Training pruned neural networks. *CoRR*, abs/1803.03635, 2018.

- [34] Colin Raffel, Noam Shazeer, Adam Roberts, Katherine Lee, Sharan Narang, Michael Matena, Yanqi Zhou, Wei Li, and Peter J. Liu. Exploring the limits of transfer learning with a unified text-to-text transformer. *CoRR*, abs/1910.10683, 2019.
- [35] Jacob Devlin, Ming-Wei Chang, Kenton Lee, and Kristina Toutanova. BERT: Pre-training of deep bidirectional transformers for language understanding. In *Proceedings of the 2019 Conference of the North American Chapter of the Association for Computational Linguistics: Human Language Technologies, Volume 1 (Long and Short Papers)*, pages 4171–4186, Minneapolis, Minnesota, June 2019. Association for Computational Linguistics.
- [36] Alec Radford, Jeffrey Wu, Rewon Child, David Luan, Dario Amodei, Ilya Sutskever, et al. Language models are unsupervised multitask learners. *OpenAI blog*, 1(8):9, 2019.
- [37] Virginia Klema and Alan Laub. The singular value decomposition: Its computation and some applications. *IEEE Transactions on automatic control*, 25(2):164–176, 1980.
- [38] Biao Zhang and Rico Sennrich. Root mean square layer normalization. *CoRR*, abs/1910.07467, 2019.
- [39] Jimmy Lei Ba, Jamie Ryan Kiros, and Geoffrey E. Hinton. Layer normalization, 2016.
- [40] Sergey Ioffe and Christian Szegedy. Batch normalization: Accelerating deep network training by reducing internal covariate shift. *CoRR*, abs/1502.03167, 2015.
- [41] Alex Wang, Amanpreet Singh, Julian Michael, Felix Hill, Omer Levy, and Samuel Bowman. GLUE: A multi-task benchmark and analysis platform for natural language understanding. In *Proceedings of the 2018 EMNLP Workshop BlackboxNLP: Analyzing and Interpreting Neural Networks for NLP*, pages 353–355, Brussels, Belgium, November 2018. Association for Computational Linguistics.
- [42] Pranav Rajpurkar, Jian Zhang, Konstantin Lopyrev, and Percy Liang. SQuAD: 100,000+ questions for machine comprehension of text. In *Proceedings of the 2016 Conference on Empirical Methods in Natural Language Processing*, pages 2383–2392, Austin, Texas, November 2016. Association for Computational Linguistics.
- [43] Seonhoon Kim, Inho Kang, and Nojun Kwak. Semantic sentence matching with densely-connected recurrent and co-attentive information. In *Proceedings of the AAAI conference on artificial intelligence*, volume 33, pages 6586–6593, 2019.
- [44] Zhiguo Wang, Wael Hamza, and Radu Florian. Bilateral multi-perspective matching for natural language sentences. *arXiv preprint arXiv:1702.03814*, 2017.
- [45] Richard Socher, Alex Perelygin, Jean Wu, Jason Chuang, Christopher D Manning, Andrew Y Ng, and Christopher Potts. Recursive deep models for semantic compositionality over a sentiment treebank. In *Proceedings of the 2013 conference on empirical methods in natural language processing*, pages 1631–1642, 2013.
- [46] William B. Dolan and Chris Brockett. Automatically constructing a corpus of sentential paraphrases. In *Proceedings of the Third International Workshop on Paraphrasing (IWP2005)*, 2005.
- [47] Hassan Sajjad, Fahim Dalvi, Nadir Durrani, and Preslav Nakov. On the effect of dropping layers of pre-trained transformer models. *Computer Speech & Language*, 77:101429, 2023.
- [48] Andrzej Maćkiewicz and Waldemar Ratajczak. Principal components analysis (pca). *Computers & Geosciences*, 19(3):303–342, 1993.
- [49] Thomas Wolf, Lysandre Debut, Victor Sanh, Julien Chaumond, Clement Delangue, Anthony Moi, Pierric Cistac, Tim Rault, Rémi Louf, Morgan Funtowicz, and Jamie Brew. Huggingface’s transformers: State-of-the-art natural language processing. *CoRR*, abs/1910.03771, 2019.
- [50] Pranav Rajpurkar, Robin Jia, and Percy Liang. Know what you don’t know: Unanswerable questions for SQuAD. In *Proceedings of the 56th Annual Meeting of the Association for Computational Linguistics (Volume 2: Short Papers)*, pages 784–789, Melbourne, Australia, July 2018. Association for Computational Linguistics.

A Architecture of Cross-Attention (CA) Layer

The CA layer consists of H attention heads, taking x as input and output x_C .

$$x_C = x + \text{CA}(\text{norm}(x)), \quad x_n = \text{norm}(x), \quad \text{CA}(x_n) = \sum_{i=1}^H \text{Att}^{(i)}(x_e, x_n), \quad (28)$$

$$\text{Att}^{(i)}(x_e, x_n) = W_O^{(i)\top} W_V^{(i)} x_e \cdot \text{Softmax}((W_K^{(i)} x_e)^\top (W_Q^{(i)} x_n) / \sqrt{d}), \quad (29)$$

where x_e is the outputs of the encoder, $\text{norm}(x)$ represents the normalization function such as LayerNorm or RMSNorm, and $W_Q, W_K, W_V, W_O \in \mathbb{R}^{d_h \times d}$ represent the parameters of the CA layer. These parameters correspond to the query, key, value, and output matrices, respectively. Here, d denotes the hidden size, and $d_h = d/H$ denotes the attention head size.

B Proof of Equation 7

Let X be a matrix formed by concatenating a series of submatrices in the following manner:

$$X = [L^{(1)}(x_1), \dots, L^{(1)}(x_M), L^{(1\sim 2)}(x_1), \dots, L^{(1\sim 2)}(x_M), L^{(1\sim N)}(x_1), \dots, L^{(1\sim N)}(x_M)]. \quad (30)$$

Then, we have,

$$\arg \min_P \mathbb{E}_{x \in \mathbb{D}} \left(\sum_{i=1}^N \|L^{(1\sim i)}(x) - PP^\top L^{(1\sim i)}(x)\|_F^2 \right) \quad \text{s.t.} \quad P^\top P = \mathbf{I} \quad (31)$$

$$\iff \arg \min_P \sum_{j=1}^M \left(\sum_{i=1}^N \|L^{(1\sim i)}(x_j) - PP^\top L^{(1\sim i)}(x_j)\|_F^2 \right) \quad \text{s.t.} \quad P^\top P = \mathbf{I} \quad (32)$$

$$\iff \arg \min_P \sum_{i=1}^N \sum_{j=1}^M \|L^{(1\sim i)}(x_j) - PP^\top L^{(1\sim i)}(x_j)\|_F^2 \quad \text{s.t.} \quad P^\top P = \mathbf{I} \quad (33)$$

$$\iff \arg \min_P \sum_{i=1}^N \sum_{j=1}^M \|X[(i-1) * M + j] - PP^\top X[(i-1) * M + j]\|_F^2 \quad \text{s.t.} \quad P^\top P = \mathbf{I} \quad (34)$$

$$\iff \arg \min_P \|X - PP^\top X\|_F^2 \quad P^\top P = \mathbf{I}, \quad (35)$$

where $M = |\mathbb{D}|$ is the number of the sampled data instances, $X[(i-1) * M + j] = L^{(1\sim i)}(x_j)$ represents the submatrix associated with the i -th layer and the j -th data instance.

Therefore, Eq. 6 is equivalent to the following equation,

$$\arg \min_P \|X - PP^\top X\|_F^2 \quad \text{s.t.} \quad P^\top P = \mathbf{I}. \quad (36)$$

The optimization problem associated with Eq. 36 corresponds to one of the formulations of Principal Component Analysis [48]. Solving this problem yields the matrix U , which is obtained through the Singular Value Decomposition (SVD) of matrix X .

C Normalization Function Approximation

LayerNorm. For LayerNorm, we have,

$$\text{norm}(x) = \gamma * \frac{x - \mathbb{E}(x)}{\sqrt{\text{Var}(x) + \epsilon}} + \beta. \quad (37)$$

Then, we have

$$\text{norm}(P\hat{x}) = \gamma * \frac{P\hat{x} - \mathbb{E}(P\hat{x})}{\sqrt{\text{Var}(P\hat{x}) + \epsilon}} + \beta \quad (38)$$

$$\approx \hat{P} * (\gamma_n * \frac{\hat{x} - \mathbb{E}(\hat{x})}{\sqrt{\text{Var}(\hat{x}) + \epsilon}} + \beta_n) + \hat{b} \quad (39)$$

$$\approx \hat{P} * \text{norm}(\hat{x}) + \hat{b}, \quad (40)$$

where $\hat{P} = \gamma * P * \gamma_n^{-1}$, $\hat{b} = \beta - P_n * \beta_n$, and γ_n, β_n can take any value as needed. Empirically, we find that replacing $\mathbb{E}(P\hat{x}), \text{Var}(P\hat{x})$ with $P\mathbb{E}(\hat{x}), \text{Var}(\hat{x})$ does not affect the model performance. Here, γ and β are learnable parameters of LayerNorm, $\mathbb{E}(x)$ represents the mean of x over hidden units, and $\text{Var}(x)$ represents the variance of x over hidden units.

BatchNorm. For BatchNorm, we have

$$\text{norm}(x) = \gamma * \frac{(x - x_{\text{mean}})}{\sqrt{x_{\text{var}} + \epsilon}} + \beta. \quad (41)$$

Then, we have,

$$\text{norm}(P\hat{x}) = \gamma * \frac{(P\hat{x} - x_{\text{mean}})}{\sqrt{x_{\text{var}} + \epsilon}} + \beta \quad (42)$$

$$= \hat{P} * (\gamma_n * \frac{\hat{x} - 0}{1} + \beta_n) + \hat{b} \quad (43)$$

$$= \hat{P} * \text{norm}(\hat{x}) + \hat{b}, \quad (44)$$

where $\hat{P} = \frac{\gamma}{\sqrt{x_{\text{var}} + \epsilon}} P \gamma_n^{-1}$, $\hat{b} = \beta - \frac{\gamma}{\sqrt{x_{\text{var}} + \epsilon}} x_{\text{mean}} - \hat{P} \beta_n$, and γ_n, β_n can take any value as needed. Here, γ and β are learnable parameters of BatchNorm, and x_{mean} and x_{var} are the mean and variance of each dimension over data instances.

D Transformer Compression with Post-Normalization

For the transformer model with a post-normalization function (e.g., BERT), each layer of the model is formalized as:

$$L_n^{(l)}(x_n) = \text{norm}^{(l)}(L^{(l)}(x_n)), \quad L^{(l)}(x_n) = x_n + \text{Layer}(x_n), \quad x_n = \text{norm}^{(l-1)}(x), \quad (45)$$

where l denotes the index of layer. We further define,

$$L^{(1 \sim i)}(x) = L^{(i)} \circ \text{norm}^{(i-1)} \dots \text{norm}^{(1)} \circ L^{(1)} \circ \text{norm}^{(0)}(x) \quad (46)$$

$$L_n^{(1 \sim i)}(x) = \text{norm}^{(i)} \circ L^{(i)} \circ \text{norm}^{(i-1)} \dots \text{norm}^{(1)} \circ L^{(1)} \circ \text{norm}^{(0)}(x). \quad (47)$$

Then given an input x , we pass it through the transformer model starting from the first layer to the last N -th layer, resulting in the corresponding feature vector,

$$L_n^{(1\sim N)}(x) = \text{norm}^{(N)} \circ L^{(N)} \circ \text{norm}^{(N-1)} \dots \text{norm}^{(1)} \circ L^{(1)} \circ \text{norm}^{(0)}(x). \quad (48)$$

According to Eq. 6, we can use the projection matrix P to add dimensionality reduction and dimensionality enhancement operations between each layer, while preserving the final output, as shown in the following equation,

$$\tilde{L}_n^{(1\sim N)}(x) \approx \text{norm}^{(N)} \circ U \circ D \circ L^{(N)} \dots \text{norm}^{(1)} \circ L^{(1)} \circ U \circ D \circ \text{norm}^{(0)}(x) \quad (49)$$

$$\approx \hat{P}^{(N)}(\text{no}\hat{\text{r}}\text{m}^{(N)} \circ \hat{L}^{(N)} \dots \text{no}\hat{\text{r}}\text{m}^{(1)} \circ \hat{L}^{(1)} \circ \text{no}\hat{\text{r}}\text{m}^{(0)}(P^\top x)) \quad (50)$$

$$\approx \hat{P}^{(N)} \hat{L}_n^{(1\sim N)}(P^\top x), \quad (51)$$

where $U(x) = Px$ represents the dimensionality enhancement operation, $D(x) = P^\top x$ represents the dimensionality reduction operation, $\hat{L}^{(i)} \circ \text{no}\hat{\text{r}}\text{m}^{(i-1)} = D \circ L^{(i)} \circ \text{norm}^{(i-1)} \circ U$ is the projected layer, and $\hat{L}_n^{(1\sim N)} = \text{no}\hat{\text{r}}\text{m}^{(N)} \circ \hat{L}^{(N)} \dots \text{no}\hat{\text{r}}\text{m}^{(1)} \circ \hat{L}^{(1)} \circ \text{no}\hat{\text{r}}\text{m}^{(0)}$ is the projected model.

For a projected layer $\hat{L}^{(i)} \circ \text{no}\hat{\text{r}}\text{m}^{(i-1)}(\hat{x})$, we have,

$$\hat{L}^{(i)} \circ \text{no}\hat{\text{r}}\text{m}^{(i-1)}(\hat{x}) = D \circ L^{(i)} \circ \text{norm}^{(i-1)} \circ U(\hat{x}) \quad (52)$$

$$= P^\top (\text{norm}^{(i-1)}(P\hat{x}) + \text{Layer}(\text{norm}^{(i-1)}(P\hat{x}))). \quad (53)$$

According to appendix C, by the approximation of the post-normalization function, we can replace $\text{norm}(P\hat{x})$ with $\hat{P}\text{no}\hat{\text{r}}\text{m}(\hat{x})$ (For the sake of simplicity, we ignore bias here). Then we have,

$$\hat{L}^{(i)} \circ \text{no}\hat{\text{r}}\text{m}^{(i-1)}(\hat{x}) \approx P^\top (\hat{P}^{(i-1)} \text{no}\hat{\text{r}}\text{m}^{(i-1)}(\hat{x}) + \text{Layer}(\hat{P}^{(i-1)} \text{no}\hat{\text{r}}\text{m}^{(i-1)}(\hat{x}))). \quad (54)$$

With matrix fusion, we can compress the Layer function to $\hat{\text{L}}\hat{\text{a}}\hat{\text{y}}\hat{\text{e}}\hat{\text{r}}$, i.e.,

$$\hat{L}^{(i)} \circ \text{no}\hat{\text{r}}\text{m}^{(i-1)}(\hat{x}) \approx P^\top \hat{P}^{(i-1)} \text{no}\hat{\text{r}}\text{m}^{(i-1)}(\hat{x}) + \hat{\text{L}}\hat{\text{a}}\hat{\text{y}}\hat{\text{e}}\hat{\text{r}}(\text{no}\hat{\text{r}}\text{m}^{(i-1)}(\hat{x})). \quad (55)$$

There is an additional matrix $P^\top \hat{P}^{(i-1)}$ in Eq. 55, where $P^\top \hat{P}^{(i-1)} = P^\top \gamma P \gamma_n^{-1}$. Since we can set the value of γ_n arbitrarily, we approximate $P^\top \gamma P$ with $\text{diag}(P^\top \gamma P)$ and set γ_n to $\text{diag}(P^\top \gamma P)$. Then, we have $P^\top \hat{P}^{(i-1)} \approx \mathbf{I}$. Therefore, we finally have,

$$\hat{L}^{(i)} \circ \text{no}\hat{\text{r}}\text{m}^{(i-1)}(\hat{x}) \approx \text{no}\hat{\text{r}}\text{m}^{(i-1)}(\hat{x}) + \hat{\text{L}}\hat{\text{a}}\hat{\text{y}}\hat{\text{e}}\hat{\text{r}}(\text{no}\hat{\text{r}}\text{m}^{(i-1)}(\hat{x})). \quad (56)$$

In our experiments, we find that compressing the first layer of the post-normalization transformer results in a significant decline in performance. Therefore, when compressing the post-normalization transformer, we choose to exclude the compression of its first layer.

E CA Layer Compression

For CA Layer, we have,

$$\hat{\text{C}}\hat{\text{A}}(\hat{x}_n) = \sum_{i=1}^H P^\top W_O^{(i)\top} W_V^{(i)} \hat{P}_e \hat{x}_e \cdot \text{Softmax}((W_K^{(i)} \hat{P}_e \hat{x}_e)^\top (W_Q^{(i)} \hat{P} \hat{x}_n) / \sqrt{d}) \quad (57)$$

$$= \sum_{i=1}^H \hat{W}_O^{(i)\top} \hat{W}_V^{(i)} \hat{x}_e \cdot \text{Softmax}((\hat{W}_K^{(i)} \hat{x}_e)^\top (\hat{W}_Q^{(i)} \hat{x}_n) / \sqrt{d}), \quad (58)$$

where $\hat{W}_O^{(i)} = W_O^{(i)} P$, $\hat{W}_V^{(i)} = W_V^{(i)} \hat{P}_e$, $\hat{W}_K^{(i)} = W_K^{(i)} \hat{P}_e$, $\hat{W}_Q^{(i)} = W_Q^{(i)} \hat{P}$. The shape of these matrices is changed from $d_h \times d$ to $d_h \times k$, retaining k/d of the original number of parameters.

F Experiment Details

F.1 Experiment Setup

To establish the baseline models, we first download the pre-trained checkpoints from the HuggingFace Transformers repository [49]. For BERT, we conduct fine-tuning on the pre-trained model for 2 epochs, employing a batch size of 16 and a learning rate of $3e-5$ for tasks in the GLUE [41] and SQuAD [42, 50] benchmarks. For T5, we fine-tune the pre-trained model for 2 epochs, using a batch size of 16 and learning rates of $1e-4$ and $3e-5$ for tasks in the GLUE [41] and SQuAD [42, 50] benchmarks, respectively. Then, we employ a sample size of 2,000 to compress the transformer model. Finally, we refine the model weight using the same settings utilized during the fine-tuning of the baseline models. Other parameters are set to the default parameters provided by the framework.

F.2 Datasets

GLUE benchmark [41] consists of various tasks related to sentence similarity calculation, sentence classification, textual entailment, and natural language inference. It includes 10 tasks, namely AX, COLA, QQP, MNLI, MRPC, QNLI, QQP, RTE, SST-2, STS-B, and WNLI. The number of training examples for each task is as follows: 1.1k, 10.7k, 432k, 5.8k, 105k, 364k, 3k, 70k, 67k, 852, respectively. For our experiment, we select the datasets QQP, MNLI, MRPC, QNLI, QQP, SST-2, and STS-B based on the data scale and previous research [8]. The SQuAD 1.1 [42] and SQuAD 2.0 [50] datasets involve question and answering tasks, each containing 88K and 130K training examples, respectively.

F.3 Comparison of TCSP with Prior Methods on BERT

Following the experimental setup of Kwon et al. [8], we compare TCSP against previous pruning methods and low-rank factorization methods for the transformer model on four GLUE tasks: QQP, QNLI, SST-2, and MRPC. It is important to note that our evaluation solely relies on the experimental results without any additional knowledge distillation. For DRONE, as the paper only reported the speed-up metric, the compression ratio is not provided. Additionally, the results for MRPC in Sajjad et al., DynaBERT, Kwon et al., FWSVD, and TFWSVD are reported in terms of accuracy instead of F1 score. Please refer to Table 6 for the detailed experimental outcomes. Our method TCSP demonstrates comparable or superior results compared to the prior methods.

F.4 Performance Comparison of Compressed T5-base with T5-small

We conduct a comparison between the compressed T5-base and T5-small models. As shown in Table 7, the compressed T5-base, having twice the number of parameters, outperforms T5-small on all datasets. In the future, we aim to delve deeper into the layer compression algorithm to ensure that the compressed T5-base and T5-small models have an equal number of layers and hidden size. This will enable a fairer and more accurate comparison between the two models.

F.5 Performance Analysis of Compressed T5-base at Various Compression Rates

Table 8 illustrates the performance of the compressed T5-base model at different compression ratios. Notably, a reduction of 25% in the hidden size can be achieved while preserving accuracy.

F.6 Performance of Compressed LLaMa

We extend the application of TCSP to large transformer models, such as LLaMa-7B. Initially, We conduct LoRA-based fine-tuning on LLaMa-7B using the Stanford Alpaca dataset. After that, we apply TCSP to compress the transformer model. To maintain the performance, we also need to conduct LoRA-based fine-tuning on the Alpaca dataset after the compression process. To evaluate the performance of the compressed model in a zero-shot setting, we test it on three commonsense reasoning datasets: PIQA, HellaSwag, and WinoGrande. The accuracy of the model is reported for these three datasets. The experimental results shown in Table 9 demonstrate that we can compress the model by 12.5% of its parameters while incurring only a 3% degradation in performance.

Table 6: Performance comparison of TCSP with previous compression methods on BERT.

	Compression rate	QQP	QNLI	SST-2	MRPC	Diff.			
Flop [9]	baseline	-	91.6	92.7	90.9	-	0	0	0
	33.3	-	89.0	92.1	88.6	-	-2.6	-0.6	-2.3
SLIP [10]	baseline	90.6	91.6	92.7	90.9	0	0	0	0
	34.4	89.7	90.7	91.7	89.9	-0.9	-0.9	-1.0	-1.0
	38.5	88.9	89.5	91.8	88.1	-1.7	-2.1	-0.9	-2.8
Sajjad et al. [47]	baseline	91.1	91.1	92.4	88.0*	0	0	0	0
	33.3	90.6	89.7	90.6	79.4*	-0.4	-1.4	-1.8	-8.6
	50.0	90.4	87.6	90.3	80.2*	-0.7	-3.5	-2.2	-7.8
DynaBERT [23]	baseline	-	-	92.9	87.7*	-	-	0	0
	25.0	-	-	92.3	86.0*	-	-	-0.6	-1.7
	50.0	-	-	91.9	86.0*	-	-	-1.0	-1.7
EBERT [11]	baseline	87.9	91.5	93.2	-	0	0	0	-
	40.0	87.5	90.2	92.2	-	-0.4	-1.3	-1.0	-
	50.0	87.9	89.6	91.6	-	-0.7	-1.9	-1.6	-
BMP [12]	baseline	91.1	-	92.7	-	0	-	0	-
	50.0	90.4	-	90.7	-	-0.7	-	-2.0	-
Kwon et al. [8]	baseline	91.0	91.4	93.6	86.3*	0	0	0	0
	30.0	90.7	90.9	93.0	86.1*	-0.3	-0.5	-0.6	-0.2
	40.0	90.4	90.0	92.5	85.3*	-0.6	-1.4	-1.1	-1.0
	50.0	89.5	88.7	91.6	83.2*	-1.5	-2.7	-2.0	-3.1
DRONE [14]	baseline	90.9	91.4	92.3	89.5	0	0	0	0
	-	90.1	89.3	90.8	88.0	-0.8	-2.1	-1.5	-1.5
FWSVD [15]	baseline	87.8	91.3	93.0	87.4*	0	0	0	0
	40.0	87.6	89.5	91.2	88.0*	-0.2	-1.8	-1.8	+0.6
TFWSVD [16]	baseline	87.8	91.3	93.0	87.4*	0	0	0	0
	40.0	86.9	90.3	91.1	89.0*	-0.9	-1.0	-1.9	+1.6
TCSP	baseline	91.1	91.4	92.2	89.9	0	0	0	0
	40.0	90.8	90.6	91.1	89.1	-0.3	-0.8	-1.1	-0.8

Table 7: Comparison of compressed T5-base with T5-small

	MNLI	QQP	QNLI	SST-2	STS-B	MRPC	SQuAD _{1.1}	SQuAD _{2.0}
T5-small	81.6	89.5	90.7	91.5	87.4	91.0	83.3	63.9
T5-base w TCSP {25%, 25%} + ft.	86.1	90.9	92.0	93.2	89.3	92.3	87.0	77.5

G Algorithm

G.1 Projection Matrix Generation

The pseudo-code of projection matrix generation is shown in Algorithm 1.

G.2 TCSP

The pseudo-code of TCSP is shown in Algorithm 2. The pseudo-code of TCSP combined with other compression methods is shown in Algorithm 3.

Table 8: Performance of compressed T5-base at different compression ratios

	MNLI	QQP	QNLI	SST-2	STS-B	MRPC	SQuAD _{1.1}	SQuAD _{2.0}
T5-base	86.8	91.4	93.2	94.5	90.0	91.9	88.6	79.3
w TCSP {12.5%, 0%} + ft.	86.5	91.2	92.6	94.4	90.3	91.0	87.2	78.1
w TCSP {25%, 0%} + ft.	86.2	91.2	92.5	93.2	90.1	91.3	86.8	78.0
w TCSP {37.5%, 0%} + ft.	84.8	90.6	92.1	92.4	89.3	91.7	86.0	76.0
w TCSP {50%, 0%} + ft.	82.6	90.5	89.9	90.9	83.4	83.4	84.4	73.9

Table 9: Performance of compressed LLaMa

	PIQA	HellaSwag	WinoGrande
LLaMa-7B+LoRa-ft.	77.4	73.9	63.2
+TCSP{12.5%, 0%}	74.3	68.0	60.7
+TCSP{12.5%, 0%}+LoRa-ft.	75.4	71.1	61.0
+TCSP{25.0%, 0%}	68.4	62.6	56.0
+TCSP{25.0%, 0%}+LoRa-ft.	72.7	63.3	59.6

G.3 TCSP-filter-pruning

The pseudo-code of TCSP-filter-pruning is shown in Algorithm 4.

G.4 TCSP-head-size-compression

The pseudo-code of TCSP-head-size-compression is shown in Algorithm 5.

H Societal Impacts

We believe that our work will not have an immediate negative impact on society, as its primary objective is to accelerate model inference without compromising the output quality.

I Limitation and Future Work

There are two key considerations regarding TCSP. Firstly, it relies on performing SVD on the feature matrix for model compression. However, the computational overhead associated with SVD and the storage requirements for the feature matrix using a limited number of samples. Secondly, our current method exclusively supports compressing of models employing the Transformer structure. In the future, we intend to delve into alternative techniques for computing the projection matrix, offering greater flexibility for handling large-scale matrices. Additionally, we aim to extend the application of our compression methods to encompass diverse model structures.

Algorithm 1: Projection Matrix Generation (PMG)

Input: r : compression ratio, T : sampled tokens size, \mathbb{D} : a subset of training data, $L^{(1\sim N)}$:
model, d : hidden size

Output: Projection Matrix P

```
X ← []
for m ← 0 to M do
  x(0) ←  $\mathbb{D}[m]$ 
  for i ← 1 to N do
    x(i) ← L(i)(x(i-1))
    xs(i) = Sample(x(i), T)
    X ← Concatenate(X, xs(i))
  end
end
U, Σ, V⊤ ← SVD(X)
k ← ⌈d * r⌉
P ← U[:,k]
```

Algorithm 2: TCSP

Input: r : compression ratio, T : sampled tokens size, \mathbb{D} : a subset of the training data

Output: Compressed model $\hat{L}^{(1\sim N)}$

$P \leftarrow \text{PMG}(r, T, \mathbb{D})$

for $i \leftarrow 1$ to $|MHA|$ do

 for $j \leftarrow 1$ to H do

$[\gamma, W_O, W_V, W_Q, W_K] \leftarrow MHA_j^{(i)}$

 ▷ Load MHA Parameters

$\hat{P} \leftarrow \sqrt{\frac{d}{k}} \gamma P$

$\hat{MHA}_j^{(i)} \leftarrow [\mathbf{I}, W_O P, W_V \hat{P}, W_Q \hat{P}, W_K \hat{P}]$

 ▷ Set MHA Parameters

 end

end

for $i \leftarrow 1$ to $|FFN|$ do

$[\gamma, W_D, W_U] \leftarrow FFN^{(i)}$

 ▷ Load FFN Parameters

$\hat{P} \leftarrow \sqrt{\frac{d}{k}} \gamma P$

$\hat{FFN}^{(i)} \leftarrow [\mathbf{I}, W_D P, W_U \hat{P}]$

 ▷ Set FFN Parameters

end

$\hat{M} \leftarrow [\hat{MHA}, \hat{FFN}]$

Algorithm 3: TCSP-combine

Input: r : compression ratio, T : sampled tokens size, \mathbb{D} : a subset of the training data

Output: Compressed model $\hat{L}^{(1\sim N)}$

$P \leftarrow \text{PMG}(r, T, \mathbb{D})$

$\text{Mask} \leftarrow \text{TFP}(r, T, \mathbb{D})$

$U_M, V_M, U_{M'}, V_{M'} \leftarrow \text{THSC}(r, T, \mathbb{D})$

for $i \leftarrow 1$ **to** $|\text{MHA}|$ **do**

for $j \leftarrow 1$ **to** H **do**

$[\gamma, W_O, W_V, W_Q, W_K] \leftarrow \text{MHA}_j^{(i)}$

$\hat{P} \leftarrow \sqrt{\frac{d}{k}} \gamma P$

$\hat{\text{MHA}}_j^{(i)} \leftarrow [\mathbf{I}, V_{M',j}^{(i)\top} W_O P, U_{M',j}^{(i)\top} W_V \hat{P}, V_{M,j}^{(i)\top} W_Q \hat{P}, U_{M,j}^{(i)\top} W_K \hat{P}]$

end

end

for $i \leftarrow 1$ **to** $|\text{FFN}|$ **do**

$[\gamma, W_D, W_U] \leftarrow \text{FFN}^{(i)}$

$\hat{P} \leftarrow \sqrt{\frac{d}{k}} \gamma P$

$\hat{\text{FFN}}^{(i)} \leftarrow [\mathbf{I}, \text{Mask}^{(i)} W_D P, \text{Mask}^{(i)} W_U \hat{P}]$

end

$\hat{L}^{(1\sim N)} \leftarrow [\hat{\text{MHA}}, \hat{\text{FFN}}]$

Algorithm 4: TCSP-filter-pruning (TFP)

Input: r : compression ratio, T : sampled tokens size, \mathbb{D} : a subset of training data, $L^{(1\sim N)}$: model, d_f : number of filters

Output: TCSP Pruning Mask Mask

$\text{E}[\text{X}]_* \leftarrow 0$

$\text{E}[\text{X}^2]_* \leftarrow 0$

for $m \leftarrow 1$ **to** M **do**

$x^{(0)} \leftarrow \mathbb{D}[m]$

for $i \leftarrow 1$ **to** N **do**

$x^{(i)} \leftarrow L^{(i)}(x^{(i-1)})$

if $L^{(i)}$ is j -th FFN Layer $\text{FFN}^{(j)}$ **then**

$\text{E}[\text{X}]_j \leftarrow \text{Update}(\text{E}[\text{X}]_j, x^{(i)})$

$\text{E}[\text{X}^2]_j \leftarrow \text{Update}(\text{E}[\text{X}^2]_j, x^{(i)} * x^{(i)})$

end

end

end

$K \leftarrow \lceil d_f * r \rceil$

for $i \leftarrow 1$ **to** $|\text{FFN}|$ **do**

$\text{E}_i \leftarrow \text{E}[\text{X}]_i$

$\text{std}_i \leftarrow \sqrt{\text{E}[\text{X}^2]_i - (\text{E}[\text{X}]_i)^2}$

$\text{Score}(\ast) \leftarrow |W_{D,\ast}| (\text{E}_{i,\ast} + \text{std}_{i,\ast})$

$\text{Index} \leftarrow \text{TopK_Index}(\text{Score}, K)$

$\text{Mask}_j \leftarrow \text{GenerateMask}(d_f, \text{Index})$

 ▷ Select Top-K important filters

 ▷ Mask_j is a $\mathbb{R}^{K \times d_f}$ matrix for pruning filters

end

$\text{Mask} \leftarrow [\text{Mask}_1, \text{Mask}_2, \dots, \text{Mask}_{|\text{FFN}|}]$

Algorithm 5: TCSP-head-size-compression (THSC)

Input: r : compression ratio, T : sampled tokens size, \mathbb{D} : a subset of training data, $L^{(1\sim N)}$:
model, d : hidden size

Output: Projection Matrices $U_M, V_M, U_{M'}, V_{M'}$

for $i \leftarrow 1$ **to** $|MHA|$ **do**

$X_K^{(i)} \leftarrow \square$

$X_Q^{(i)} \leftarrow \square$

$X_V^{(i)} \leftarrow \square$

end

for $m \leftarrow 0$ **to** M **do**

$x^{(0)} \leftarrow \mathbb{D}[m]$

for $i \leftarrow 1$ **to** N **do**

$x^{(i)} \leftarrow L^{(i)}(x^{(i-1)})$

if $L^{(i)}$ is j -th MHA Layer $MHA^{(j)}$ **then**

$x_s^{(i)} = \text{Sample}(x^{(i)}, T)$

$X_Q^{(j)} \leftarrow \text{Concate}(X_Q^{(i)}, W_Q^{(j)} x_s^{(i)})$

$X_K^{(j)} \leftarrow \text{Concate}(X_K^{(i)}, W_K^{(j)} x_s^{(i)})$

$X_V^{(j)} \leftarrow \text{Concate}(X_V^{(i)}, W_V^{(j)} x_s^{(i)})$

end

end

end

for $i \leftarrow 1$ **to** N **do**

if $L^{(i)}$ is j -th MHA Layer $MHA^{(j)}$ **then**

\triangleright Solve Eq.26 and Eq.27 for each head

for $k \leftarrow 1$ **to** H **do**

$U_{M,k}^{(j)}, V_{M,k}^{(j)}, U_{M',k}^{(j)}, V_{M',k}^{(j)} \leftarrow \text{Solve}_k(X_Q^{(j)}, X_K^{(j)}, X_V^{(j)})$

end

end

end

$U_M \leftarrow [U_M^{(1)}, U_M^{(2)}, \dots, U_M^{(|MHA|)}]$

$V_M \leftarrow [V_M^{(1)}, V_M^{(2)}, \dots, V_M^{(|MHA|)}]$

$U_{M'} \leftarrow [U_{M'}^{(1)}, U_{M'}^{(2)}, \dots, U_{M'}^{(|MHA|)}]$

$V_{M'} \leftarrow [V_{M'}^{(1)}, V_{M'}^{(2)}, \dots, V_{M'}^{(|MHA|)}]$
